

Showcasing research from Jungmok Seo's laboratory,  
School of Electrical and Electronic Engineering,  
Yonsei University, Seoul, Republic of Korea.

Liquid-based electronic materials for bioelectronics: current  
trends and challenges

Liquid-based electronic materials take bioelectronics a step  
forward to a seamlessly integrated human-machine interface  
owing to their conformability, durability, biocompatibility  
and flexibility.

### As featured in:



See Jungmok Seo *et al.*,  
*Ind. Chem. Mater.*, 2024, 2, 361.

## REVIEW

View Article Online  
View Journal | View Issue



Cite this: *Ind. Chem. Mater.*, 2024, 2, 361

# Liquid-based electronic materials for bioelectronics: current trends and challenges

Kijun Park,<sup>a</sup> Sangwoo Park,<sup>a</sup> Yejin Jo,<sup>ab</sup> Soo A. Kim,<sup>a</sup> Tae Young Kim,<sup>a</sup> Sangwon Kim<sup>a</sup> and Jungmok Seo <sup>\*ab</sup>

Liquid-based materials have emerged as promising soft materials for bioelectronics due to their defect-free nature, conformability, robust mechanical properties, self-healing, conductivity, and stable interfaces. A liquid is infiltrated into a structuring material endowing the material with a liquid-like behavior. Liquid-based electronics with favorable features are being designed and engineered to meet requirements of practical applications. In this review, various types of liquid-based electronic materials and the recent progress on bioelectronics in multiple applications are summarized. Liquid-based electronic materials include ionic liquid hydrogel, nanomaterial-incorporated hydrogel, liquid metal, liquid-infused encapsulation, and liquid-based adhesive. These materials are demonstrated *via* electronic applications, including strain sensor, touch sensor, implantable stimulator, encapsulation, and adhesive as necessary components comprising electronics. Finally, the current challenges and future perspective of liquid-based electronics are discussed.

Keywords: Bioelectronics; Liquid metal; Soft electronics; Hydrogel electronics; Lubricant-infused.

Received 14th November 2023,  
Accepted 19th February 2024

DOI: 10.1039/d3im00122a

rsc.li/icm

## 1 Introduction

Soft electronics have been emerging as an alternative to traditional rigid and solid-based electronics due to their

superior mechanical compliance and deformability.<sup>1–4</sup> In particular, soft electronics have been extensively investigated in biomedical applications due to their capability to monitor and manage patients' bio-signals.<sup>5–9</sup> Soft electronic devices should be capable of detecting bio-signals which include electrophysiological signals, physical signals, and biochemical signals while being integrated into the human body.<sup>10–12</sup> However, existing solid-based electronic materials

<sup>a</sup> School of Electrical and Electronic Engineering, Yonsei University, Seoul 03722, Republic of Korea. E-mail: Jungmok.seo@yonsei.ac.kr

<sup>b</sup> Lynk Solutech Inc., Seoul 03722, Republic of Korea



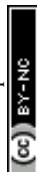
Kijun Park

Kijun Park is a graduate student in the electrical and electronic engineering department at Yonsei University. He received his bachelor's degree in material science at the University of New South Wales. His research has been focused on interface engineering between biological tissues and biomaterials, and their application in bioelectronics.



Jungmok Seo

Jungmok Seo is an associate professor in the electrical and electronic engineering department at Yonsei University. He received his bachelor's and Ph.D. degrees in electrical and electronic engineering at Yonsei University. He served as a postdoctoral research fellow at Brigham and Women's Hospital and Harvard Medical School. His research has focused on the development of functional systems for biointegrative applications using a nature-inspired approach. He is working on the development of bioelectronic devices based on liquid-based electronic materials to overcome existing limitations in solid-based bioelectronics, including longevity, infection, and immune-related side effects.





are mechanically mismatched with human tissues which hinders the stable integration between them.<sup>13–15</sup> The rigid and bulky electronic materials cause poor mechanical compliance and discomfort limiting device performances.<sup>16–18</sup> Moreover, solid-based electronic materials are prone to external stimuli including moisture,<sup>19</sup> and mechanical damages,<sup>20</sup> causing device malfunction and shortening of the lifespan.<sup>21</sup>

To overcome the challenges present in solid-based electronics, various attempts have been made to match the mechanical disparity between solids and tissues. Structural designs including wrinkled and serpentine designs were implemented to impart flexibility to electronic devices.<sup>22–24</sup> Despite the improved flexibility, the devices are prone to repeated mechanical deformations that exceed a threshold resulting in performance degradation and failure.<sup>25,26</sup> The limitations promote the needs of self-healing or self-repairing capabilities to withstand mechanical damages.<sup>10</sup> As potential candidates having conductivity, conformability, and self-healing properties, liquid-based materials have attracted researchers' attention to overcome the challenges.<sup>27</sup> For example, there are liquid-based soft electronics using ionic liquid-based ionic hydrogels, conductive hydrogels, and liquid metals.<sup>28–32</sup> Moreover, liquid-based materials have been widely adopted in adhesive strategies and encapsulations owing to their conformability and defect-free properties.

In this perspective, we summarize the recent approaches in liquid-based electronics to overcome the challenges present in the current electronics. Initially, liquid-based materials that are widely adopted are introduced, and then we describe the benefits of using them as fundamental components to impart various functionalities. Furthermore, various strategies to apply these liquid-based materials in electronic applications to achieve multi-functionality and mechanical tolerance are introduced. Moreover, liquid-based encapsulating and adhesive materials to ensure interfacial stability and device safety in harsh conditions are described with their advantages and drawbacks compared to traditional materials. Finally, limitations and future perspectives regarding liquid-based electronics are discussed.

### 1.1 Definition of liquid-based materials

Liquid-based materials have received significant attention as candidate materials to overcome the limitations of conventional materials. As liquid-based materials have significant advantages in conformability, robust mechanical properties, self-healing, defect-free nature, conductivity and stable interfaces, they have been widely adopted in various fields of studies to develop state-of-the-art soft electronics (Fig. 1). Over the last few decades, significant improvements have been achieved to narrow the mechanical differences between electronic materials and human tissues using liquid-based materials leading to various biomedical applications using soft electronics.<sup>33–35</sup> These liquid-based materials

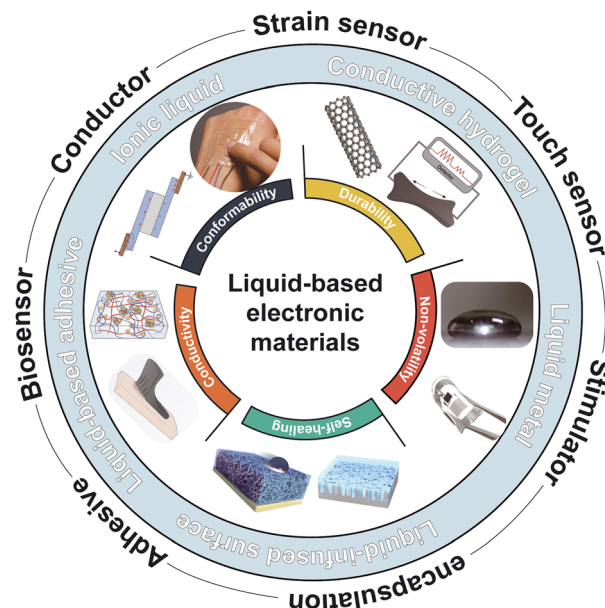


Fig. 1 Characteristics of liquid-based electronic materials, including ionic liquid, conductive hydrogel, liquid metal, liquid-infused surface, and liquid-based adhesive, and their versatile applications in bioelectronics.

exhibit liquid-like interfaces which allow formation of conformal contact with biological tissues. Moreover, they are flexible and mechanically durable to endure dynamic operational environments as soft electronics. In this review, we introduce various types of liquid-based materials that are widely used in soft electronics research, comprising ionic hydrogels, liquid metals, conductive hydrogels, liquid-infused surfaces and liquid-based adhesives, and their applications.

## 2 Liquid-based conductors

### 2.1 Ionic liquid-based materials

Ionic liquids are liquid conductors that are made of organic cations and organic or inorganic anions.<sup>36</sup> The ionic liquid-based conductor has received considerable attention due to favorable characteristics such as electrochemical window, negligible volatility, and high thermal stability. Moreover, ionic liquid-based soft electronics could possess flexibility and elasticity that is comparable to that of the skin through various chemical modifications.<sup>37,38</sup> As a promising application, ionic skin has been introduced as an artificial skin or interface that mimics the properties of human skin replicating favorable features and functionalities of human skin.

Sun *et al.* fabricated ionic skin using a polyacrylamide hydrogel, and a commercially available acrylic elastomer (VHB 4905, 3M) as a dielectric for strain sensing (Fig. 2a).<sup>30</sup> By using commercially available double-sided tape, the fabricated ionic skin was able to be attached to a finger without any debonding. The viscoelastic property of the ionic skin allows conformal contact and adhesion to dynamic and



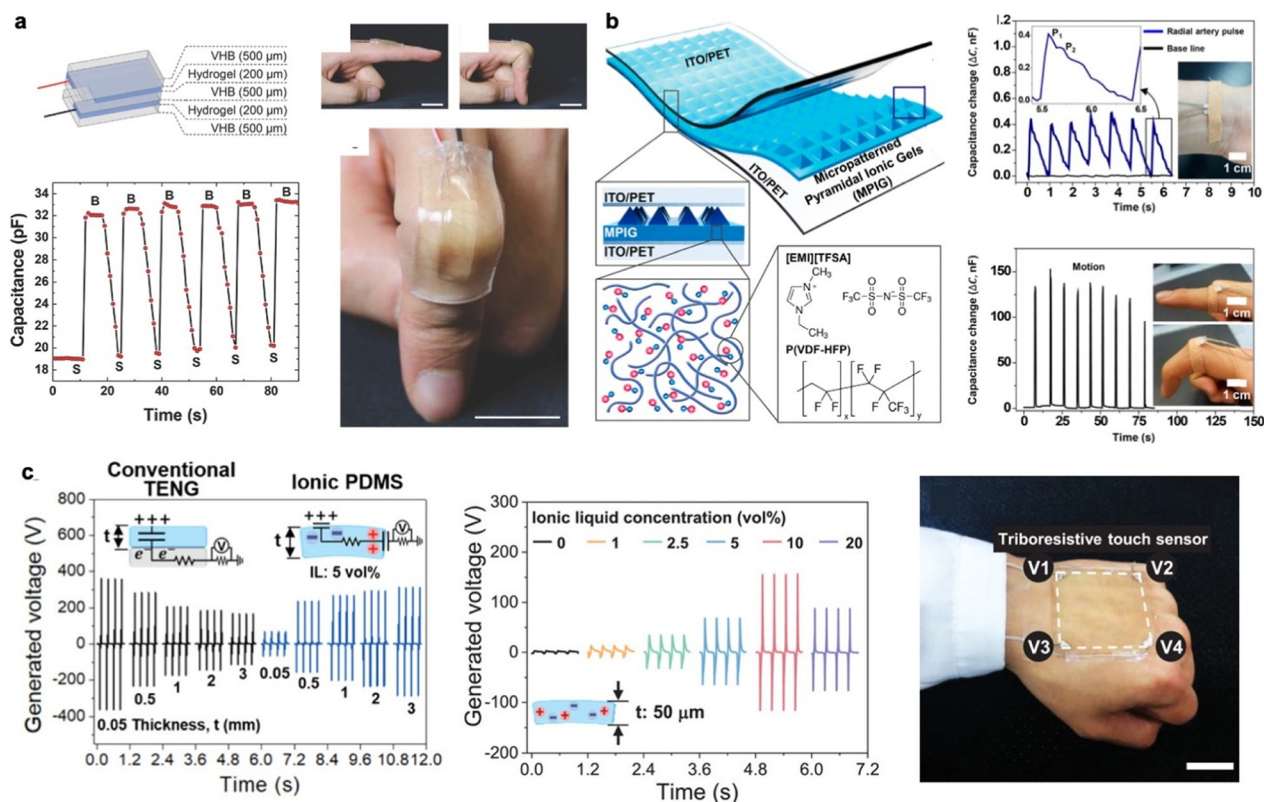


**Fig. 2** Ionic liquid-based electronics. (a) Schematic representation of the structure of ionic skin, and its capacitive changes upon hinge movement of a finger (reproduced with permission from ref. 30. Copyright 2014 John Wiley and Sons). (b) Schematic illustration of micropatterned pyramidal ionic gels sandwiched between electrodes, and their chemical structures demonstrating sensitive sensing of artery pulse and hinge movement via measuring capacitive changes (reproduced with permission from ref. 39. Copyright 2017 American Chemical Society). (c) Triboelectric generation via ionic PDMS and its application in a grid-less triboresistive touch sensor (reproduced with permission from ref. 41. Copyright 2022 John Wiley and Sons).

curved surfaces which enable more accurate strain sensing. Using the ionic skin sensor, capacitance was measured with the capacitance tuned to a sinusoidal measurement signal of 1 V and 100 Hz while the finger bent repeatedly. To avoid evaporation of ionic liquid during the experiment, the ionic hydrogel was encapsulated with VHB which resulted in stable adhesion to the finger even after massive deformation. To improve the sensing capability of the ionic hydrogel, structural design was implemented by Cho *et al.*<sup>39</sup> They used PVDF-HFP as a structuring polymer and 1-ethyl-3-methylimidazolium bis(trifluoromethylsulfonyl)amide ([TFSA]) as the ionic liquid and fabricated a pyramidal-shaped ionic gel (Fig. 2b). Then, the topographical micropatterned hydrogels were sandwiched by two electrodes resulting in periodic air gaps. This allows highly sensitive measurements for a wide range of pressures up to 50 kPa, with a sensitivity of more than 2 kPa<sup>-1</sup>. In this work, the measurement of artery pulse and the strain made by finger movement were demonstrated. Furthermore, ionic liquid hydrogels can be utilized in energy harvesting devices, especially in a triboelectric nanogenerator (TENG).<sup>40</sup> The TENG was fabricated using ionic hydrogel based on a crosslinked poly(vinyl alcohol) (PVA) and VHB tape as a substrate. An electrical double layer was formed out of these

two components to enhance the energy-harvesting performance. The important aspect of the ionic skin-based TENG is mechanical stability. Compared to a conventional TENG made of silicone rubber, the ionic skin-based TENG can be stretched up to 700% without any performance degradation owing to the non-Newtonian behavior of the liquid-based conductor. The highly stretchable properties allow it to be used as a reliable power source under dynamic conditions. To truly behave like human skin, the touch sensor should be able to detect the touch signal without a grid. The grid-less triboresistive touch sensing was introduced using ionic skin which is known to mimic characteristics of human skin (Fig. 2c).<sup>41</sup> To realize triboresistive touch sensing, PDMS was engineered to form hydrogen bonds with an ionic liquid *via* introducing hydroxyl groups into PDMS. A touch on the ionic PDMS results in a triboelectric effect generating electricity. The generated voltage at each corner of the PDMS relies on resistance between the touch points and each corner, which ensures grid-less touch sensing. Owing to the material characteristics of PDMS, the ionic PDMS exhibits high transparency (96.5%), stretchability (539.1%), and resilience (99.0%). Despite the versatility and biocompatibility of ionic liquid-based materials, there are limitations in durability, scalability, and

electrical conductivity for use as main electrical conductors. Moreover, the evaporation of the ionic liquid also hinders practical applications.

## 2.2 Nanomaterial-incorporated conductive hydrogels

In order to achieve highly conductive and functional electronic devices, incorporation of nanomaterials instead of metal ions has been widely adopted.<sup>42–45</sup> The characteristics of a conductive hydrogel can be dependent on its composition and the additives can be mainly divided into metal-based nanomaterials and carbon nanomaterials. The excellent electrical conductivity and unique magnetic,<sup>46</sup> chemical and mechanical properties make them suitable to be used as conductive nanomaterials.<sup>47,48</sup> These exceptional characteristics render them highly versatile, finding applications in diverse fields such as light, electricity, catalysts, antibacterial agents, biosensors, and biomedicine. Moreover, metal-based nanomaterials serve as effective nano-fillers for creating conductive pathways throughout hydrogel networks due to their inherent conductivity. A notable study conducted by Xu and colleagues involved the synthesis of a stretchable and conductive hydrogel with incorporated silver nanofibers for a capacitive strain sensor.<sup>49</sup> This capacitive hydrogel strain sensor operated on a similar sensing principle to resistive strain sensors, wherein its capacitance decreased as the hydrogel stretched. The incorporated silver nanofibers provide the

hydrogel with remarkable sensitivity to deformation, achieving a maximum gauge factor (GF) of 165, significantly higher than that of conventional ionic conductive hydrogels with GF less than 10. However, it is essential to note that stable electrical signal changes were observed only within a limited deformation range (cycling stretch between 50% and 150%), as effective signals could not be obtained at cyclic tensile deformations exceeding 400%. Fig. 3a demonstrates the fabrication of a novel electrically conductive hydrogel composite with exceptional properties.<sup>50</sup> The hydrogel is synthesized with polyacrylamide (PAAm)–alginate and low concentration of silver (Ag) flakes to achieve electrical conductivity through percolation forming conductive pathways. The composite exhibits high electrical conductivity ( $374 \text{ S cm}^{-1}$ ) and a low Young's modulus ( $<10 \text{ kPa}$ ) that is comparable to that of soft adipose tissue. Moreover, the hydrogel is resistant to stretching which remains stable up to 250% strain. Despite its low metallic filler content, the hydrogel displays minimal hysteresis during cyclic loading and unloading. The mechanical robustness and high electrical conductivity suggest its potential applications in soft robotics, bioelectronics, and wearable electronics. Additionally, Liu *et al.* developed an ultra-sensitive tactile sensor using silver nanowires, graphene oxide, calcium chloride, and PVA.<sup>51</sup> The optimized concentration of these components resulted in a conductive hydrogel with an impressive GF of approximately 3500 at repeated application of 50% strain. The sensitivity of the sensor was improved by four orders of magnitude far

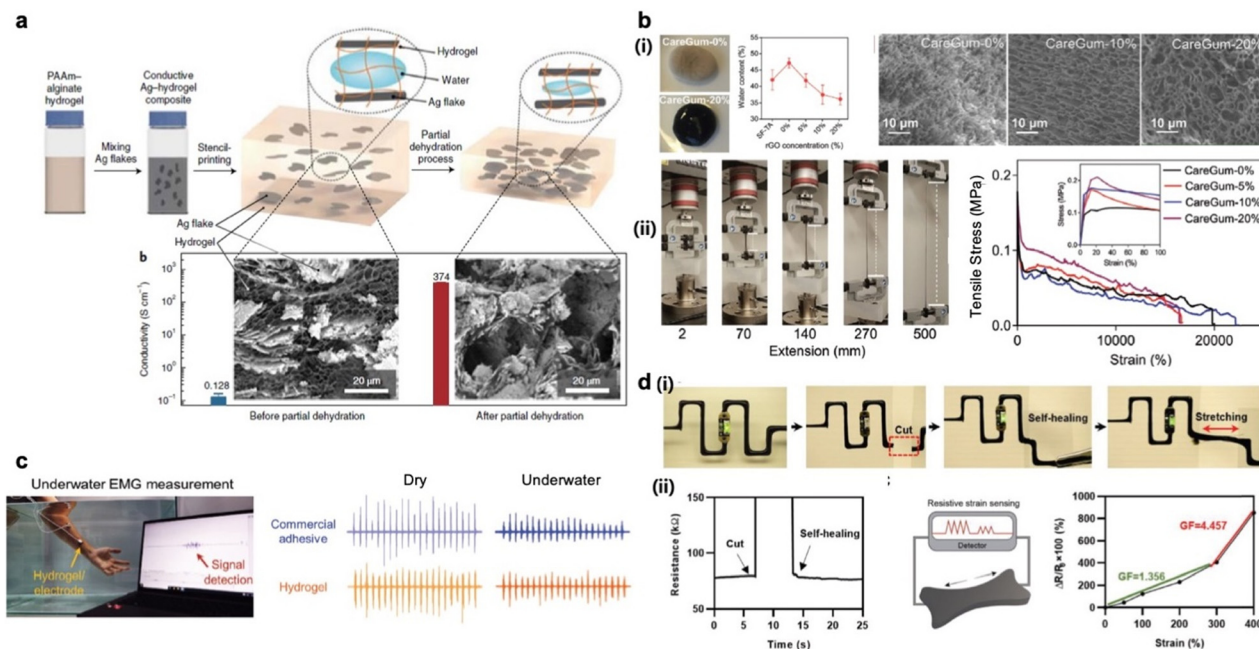


**Fig. 3** Nanomaterial-incorporated conductive hydrogels. (a) Fabrication of a conductive hydrogel comprising metallic fillers, Ag flakes, and PAAm–alginate hydrogel matrix (reproduced with permission from ref. 50. Copyright 2021 Springer Nature). (b) (i) (ii) Mechanical properties displayed through optical images and stress–strain curves of typical CareGum (reproduced with permission from ref. 53. Copyright 2021 John Wiley and Sons). (c) (i) Fabrication process of PVA/TA/PAA hydrogel with incorporated fCNT. (ii) Electromyographic (EMG) signal measurements using both a commercial adhesive and the developed CNT-based hydrogel in both dry and underwater conditions (reproduced with permission from ref. 57. Copyright 2023 John Wiley and Sons). (d) (i) 3D printed circuit with conductive hydrogel incorporating CNT (carbon nanotube) nanofillers. (ii) Application for resistive strain sensing with conductive hydrogel (reproduced with permission from ref. 58. Copyright 2023 AccScience Publishing.)





exceeding the sensitivity of pure ionic hydrogels. This heightened sensitivity enabled the accurate detection and monitoring of minute strains, allowing applications such as precise wrist pulse detection. The sensing capability allows it to distinguish various components of the pulse waveform.

A 2D carbon nanomaterial, graphene, stands out as an exceptional conductive filler due to its high surface-to-volume ratio and excellent electrical conductivity. Lv *et al.* introduced a novel approach for fabricating strain sensors utilizing graphene nanomaterial.<sup>52</sup> They coated graphene onto a hydrogel's surface to form a uniform graphene film. This method resulted in a highly sensitive composite material of graphene and hydrogel, displaying significant responsiveness to strain. For instance, the  $\Delta R/R_0$  (change in resistance relative to initial resistance) of the hydrogel reached 60% when stretched to approximately 25%. However, the graphene coating is vulnerable to extensive strain over 25% which could cause cracks leading to unstable signal recording. Kadumudi and colleagues have developed a unique self-healing hydrogel by incorporating tannic acid (TA) into silk-reduced graphene oxide (GO), designed specifically for bionic gloves (Fig. 3b(i)).<sup>53</sup> SEM images demonstrate that the porous structure depends on the proportion of reduced GO. TA, rich in hydroxyl groups, lends the hydrogel remarkable intrinsic self-healing capabilities through robust hydrogen bonding. Additionally, the self-healing properties can be attributed to reversible electrostatic and weak hydrogen bond that effectively dissipate applied stress, which results in high toughness as well (Fig. 3b(ii)). The hydrogel's outstanding self-healing ability was demonstrated *via* its recovery within 2 minutes after fracturing and stretching up to approximately 2400% after healing. The fabricated conductive hydrogel exhibited a conductivity of  $1 \text{ S m}^{-1}$ , and such an exceptional electrical conductivity allows promising applications in bionics, soft robotics and flexible bioelectronics.

Carbon nanomaterials, carbon-based materials with 3D nanostructure, have found various bioelectronic applications due to their high electrical conductivity, large surface-to-volume ratio, chemical and mechanical stability, and ease of functionalization. Unmodified CNT lacks surface functional groups, which leads to poor dissolution and dispersion in solvents hindering practical applications.<sup>54</sup> To address this challenge, researchers have functionalized CNT surfaces to add functional groups, including carboxyl and amino groups to make it promising candidate for conductive hydrogel fillers. The Gao group, for instance, functionalized multi-walled carbon nanotubes (C-MWCNTs) with carboxyl functional groups, and fabricated a hydrogel with chemical/physical crosslinking.<sup>55</sup> To fabricate the hydrogel, chitosan was used to crosslink with C-MWCNTs *via* dynamic ionic bonding. This allows the resultant hydrogel to exhibit stable signal recording under stretching. Additionally, the incorporation of the nanomaterial induced physical crosslinking throughout the hydrogel allowing effective energy dissipation and leading to self-healing and self-recovery properties. Moreover, high conductivity of the C-MWCNTs endowed the hydrogel with an exceptional electrical conductivity of  $\sim 1 \text{ S m}^{-1}$  at a concentration of 1.25 wt%. This

strategy suggests that nanomaterial incorporation could enhance the mechanical and electrical properties of the hydrogel rendering it suitable for bioelectronic applications. Another strategy that uses modified CNT was demonstrated by Lu *et al.* in which CNT was functionalized with amine- and carboxyl-rich polydopamine. The functionalized CNT was incorporated into p(AAc-co-AAM) to fabricate a conductive and adhesive hydrogel.<sup>56</sup> The CNT endowed the hydrogel with high electrical conductivity and adhesive properties even under extreme temperature ranging from  $-20$  to  $60^\circ\text{C}$ . Specifically, at 10 wt% PDA-CNTs with 50 vol% glycerol content, the hydrogel displayed a maximum conductivity of  $8.2 \text{ S m}^{-1}$  and an adhesion strength of  $57 \pm 5.2 \text{ kPa}$ . Furthermore, increasing the CNT concentration enhanced the mechanical robustness of the hydrogel in which it could endure tensile stress of 60 kPa. Dopamine modification of CNTs proved effective in improving their dispersion and reducing their agglomeration in the hydrogel, thereby enhancing the hydrogel's conductivity with increasing CNT content. In order to improve the electrical conductivity and mechanical robustness of the hydrogel, CNTs can be modified by adding carboxyl and hydroxyl functional groups and then incorporated into hydrogel. Park *et al.* synthesized a functionalized CNT-incorporated PVA/tannic acid/PAA hydrogel with improved conductivity ( $40 \text{ S m}^{-1}$ ).<sup>57</sup> The conductive hydrogel exhibits Young's modulus that is comparable to that of tissue (10 to 100 kPa) with impressive toughness ( $400\text{--}873 \text{ J m}^{-3}$ ) and stretchability ( $\sim 1000\%$  strain) (Fig. 3c). Moreover, the excellent energy dissipation *via* CNTs confined throughout the hydrogel structure promotes rapid self-healing behavior. The hydrogel could be utilized in measuring electromyography (EMG) while adhered to skin surface suggesting its potential for practical applications. Furthermore, Kim *et al.* fabricated an electronic circuit based on a conductive hydrogel incorporated with functionalized CNTs (Fig. 3d).<sup>58</sup> The hydrogel possesses a reversible hydrogen bond-based double network that makes it a viscoelastic ink. Thus, the polymer shows shear-thinning behavior allowing excellent printability with sub-micron high resolution. The practical usage of the hydrogel-based conductive ink was realized by fabricating a strain sensor by 3D printing. Nanomaterial incorporation into hydrogels has been widely adopted for improved electrical conductivity and mechanical robustness. As conductive hydrogels advanced, not only were electrically conductive hydrogels achieved, but also various characteristics including 3D printing, self-healing, and adhesion improved their usability in bioelectronic applications. Nonetheless, poor electrical conductivity compared to traditional electronic components remains as a limitation to be resolved.

### 2.3 Liquid metal-based materials

Liquid metals (LM) are metals and metal alloys that possess the properties of both liquid and metal at or near room temperature. These materials have been gaining significant attention recently due to their unique properties, possessing characteristics of both metal and liquid simultaneously.<sup>59</sup>



Mercury, which has a melting point of  $-38\text{ }^{\circ}\text{C}$ , is the only stable liquid metal at room temperature but due to its toxicity it is excluded from this article. On the other hand, gallium (Ga) has low toxicity compared to mercury which has the potential to be utilized in the field of biodevices. Liquid metals can be utilized as liquid conductors to fabricate various soft electronic devices due to excellent conductivity and deformability. Unlike solid-based electronics, which are rigid and vulnerable to mechanical deformation, liquid metal-based electronics can benefit from their unique properties. For example, a biomimetic electrochemical eye was realized using nerve fibers made of liquid metals (Fig. 4a).<sup>60</sup> Previously, biomimetic neural fibers were fabricated using metal-based fibers. However, in this work, liquid metal was used as flexible liquid conductor in soft rubber tubes for signal transmission between the nanowires, and flow characteristics of the liquid metal improved the contact resulting in clear signal transmission. The liquid characteristics and conductivity of liquid metals could greatly improve soft electronics, particularly for piezoelectric applications. Yun *et al.* used EGain microdroplets and magnetic microparticles to fabricate a liquid-metal-filled magnetorheological elastomer (LMMRE) (Fig. 4b(i)).<sup>61</sup> Compared to previously reported conductive elastic composites which exhibited conductivity decrease under strain, LMMRE demonstrates an unconventional positive piezoconductive effect in which its resistivity reaches its maximum in the relaxed state and drops dramatically under deformation. Using these characteristics, researchers demonstrated its application in wearable heating devices (Fig. 4b(ii)).

Liquid metal provides another degree of freedom in fabrication processes.<sup>62</sup> The simplest fabrication method can be simply done by injecting liquid metals into channels. Since the liquid metals can maintain their structures and functions in a stable manner due to the oxidation skin, various printing methods can be also applied to fabricate them into electrodes, including screen printing,<sup>63</sup> 3D printing,<sup>64–66</sup> nanotip printing,<sup>67</sup> and suspension printing.<sup>68</sup> Wu *et al.* fabricated a multi-mode TENG using silicone elastomer and LM.<sup>69</sup> Due to fluidity of the LM and flexibility of the silicone substrate, the TENG achieved highly stretchable and conductive characteristics at the same time, while ensuring conformal contact with skin. The TENG could sense biomechanical movements and convert them into electrical energy as an energy harvester. Moreover, the conformal contact and stretchability of the device enabled on-skin applications including exercise monitoring. Gao *et al.* designed a diaphragm pressure sensor based on a microfluidic tactile sensor (Fig. 4c(i)).<sup>70</sup> The liquid metal was simply injected into the fabricated microchannels having liquid metal sensor design with  $70\text{ }\mu\text{m}$  width and height. This allows highly sensitive, linear, low-limit-of-detection and high-resolution sensing of pressure for tactile sensing (Fig. 4c(ii)). Dickey *et al.* demonstrated a rheological behavior of LM in microchannels to achieve stable microstructures.<sup>71</sup> In this study, the flow behavior of LM is shown to be dominated by the surface characteristics of gallium oxide,

and that a critical surface stress of  $0.5\text{ N m}^{-1}$  is required for LM flow. This study provides a guide for future works using LM-based microchannels to have stable performance. Furthermore, another study was conducted to fabricate a sophisticated liquid-metal-based strain sensor with capability of wireless data transmission (Fig. 4d(i)).<sup>72</sup> The highly sensitive strain sensor offers wireless monitoring of human motions which include movements of wrist and vocal cords recognizing swallowing and speaking (Fig. 4d(ii)). The outcome demonstrates that the liquid metal can be fabricated into sophisticated patterns *via* lithography so as to be miniaturized, thin, and fully wireless. Despite the fluidity of liquid metal being beneficial for flexibility, the fluidity can be a hurdle while printing a pattern. Moreover, sophisticated designs of circuits may cause unwanted merging of the liquid metal lines due to the high surface tension leading to electrical shorting.<sup>73</sup> Despite the potential disadvantage of the fluidity of LM, Shen *et al.* utilized the fluidity and low gas permeability of LM to form hermetic and stretchable sealing for a battery and heat transfer system. Conventional soft electronic materials have a highly permeable nature, limiting their applications in packaging. In this study, the LM was used as a spacer allowing stable battery capacity of 72.5% after 500 cycles. This approach broadened the application of LM not only as an electronic conductor, but also as a sealing agent for various electronic devices. Another breakthrough was introduced by Lee *et al.* by demonstrating rapid fabrication of liquid metal circuits on various substrates *via* meniscus-guided printing (Fig. 4e).<sup>74</sup> During the fabrication processes, a nozzle forms a meniscus between the substrates, moving in accordance with the circuit designs. At this point, the solvent gets evaporated at the meniscus which results in the thin-film deposition of the liquid metal leading to printed electrodes. The resolution can reach up to  $50\text{ }\mu\text{m}$  attributed to the meniscus-guided printing allowing various soft electronic applications including EMG and ECG sensors. Furthermore, use of the photolithographic technique with LM was investigated to achieve high-resolution patterning of LM.<sup>75</sup> For the achievement of fine resolution of the LM conductive track, the intermetallic wetting behavior between LM and gold was utilized.<sup>76</sup> For the track formation, gold was patterned *via* photolithography, then the LM removed of its oxide was layered on the pattern for touch transfer. This method allowed achieving a pattern width of  $1.3\text{ }\mu\text{m}$  which demonstrates high-quality and high-resolution patterning capability of LM. Despite the high electrical conductivity of liquid metal and its applications, there are still limitations in terms of mechanical durability for its use as an electrical conductor. The loss of electrical properties is irreversible once the electrode gets separated, and an oxidation layer forms between the separated interfaces. Furthermore, high surface tension might cause merging when used at the micro- and nanoscale.

To overcome these hurdles, there have been attempts to combine nanomaterials and liquid metals to improve stability while not compromising electrical conductivity. The



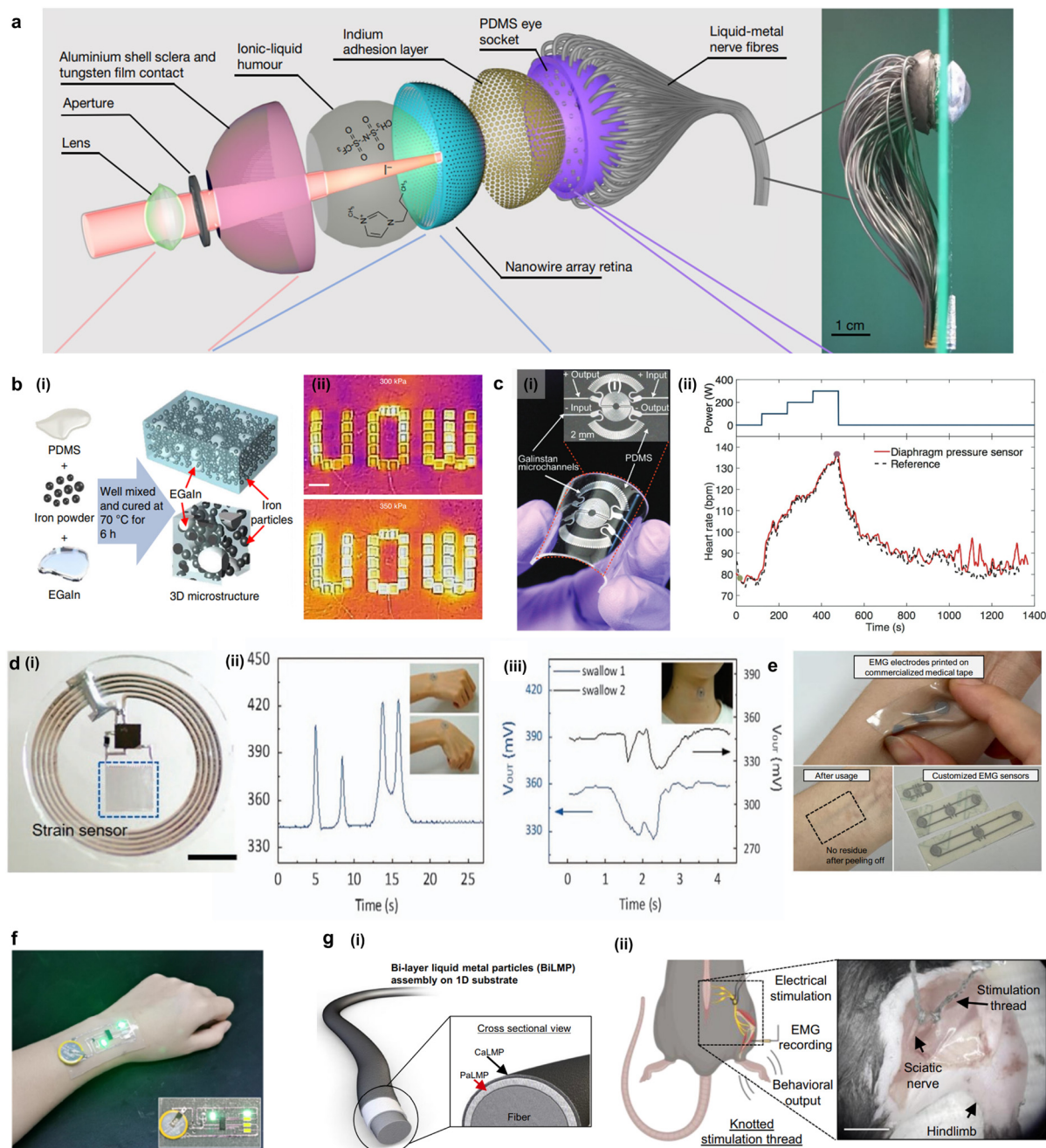


**Fig. 4** Liquid metal-utilizing biodevices. (a) Exploded view of a biomimetic eye utilizing liquid metal as nerve fibers and optical image of biomimetic eye with liquid metal nerve fibers (reproduced with permission from ref. 60. Copyright 2020 Springer Nature). (b) (i) Schematic of liquid metal magnetorheological elastomer (LMMRE). (ii) Using LMMRE to induce Joule heating effect on the device (reproduced with permission from ref. 61. Copyright 2019 Springer Nature). (c) (i) Optical image of LM-diaphragm sensor using liquid metal as microchannel. (ii) Heart-beat rate measured by the pressure sensor and a commercial reference monitoring during exercise (reproduced with permission from ref. 70. Copyright 2017 John Wiley and Sons). (d) (i) Optical image of LM-NFC device which uses liquid metal as inductor. (ii) Wireless detection of wrist motion using LM-NFC device. (iii) Real-time monitoring of muscle motion of swallowing using LM-NFC device (reproduced with permission from ref. 72. Copyright 2017 Springer Nature). (e) Optical image of deformable EMG sensor fabricated using polyelectrolyte-attached liquid metal particle (PALMP)-based ink (reproduced with permission from ref. 74. Copyright 2022 Springer Nature). (f) Photograph of temperature sensor made of liquid metal circuits using Mxene-doped liquid metal as adhesion interface (reproduced with permission from ref. 81. Copyright 2023 Springer Nature). (g) (i) Schematic illustration of bi-layer liquid metal particles (BILMP) coated on flexible fiber. (ii) *In vivo* application of BILMP coated fiber on sciatic nerve for electrical stimulation and EMG recording (reproduced with permission from ref. 79. Copyright 2023 American Chemical Society).

addition of nanomaterials brings various changes in liquid metal composites.<sup>77</sup> For example, Wang *et al.* reported a

galvanic replacement mechanism which allows the formation of graphene and LM mixture.<sup>78</sup> Due to the high surface





tension of the LM, it is difficult to form a thorough mixture. However, in this study, they used one-step ultrasonification to form reduced graphene/LM frameworks using reducing or stabilizing agents to the core. The graphene/LM frameworks displayed excellent conductivity, ion permeability, as well as capability of electrochemical detection. Conventional soft electronics are known to have poor interconnection to rigid parts of electronics due to mechanical disparity between them. Also, lack of adhesive properties of electrodes leads to unstable interconnection. As a solution, Li *et al.* demonstrated a fabrication of stable solid-liquid interconnects using a Mxene-doped liquid metal, which exhibits high electrical conductivity and adhesion force (Fig. 4f).<sup>79</sup> The low doping concentration of MEGaIn contributes to the improved fluidity of the quasi-liquid component, enabling the stretching of the interconnect line. On the other hand, the high doping concentration of MEGaIn enhances the adhesion of the quasi-solid component with the chip pins, even under high stretching conditions. Notably, this high doping concentration ensures excellent conductivity, reaching  $2.2 \times 10^6 \text{ S m}^{-1}$ . To investigate the feasibility of MEGaIn as a liquid interconnect for traditional electronic components, the MeGaIn was used to attach to resistors, light-emitting diodes (LEDs), Bluetooth chips, and microcircuit boards exhibiting stable and reliable adhesion. For realizing flexible electronic devices using LM, elastomers were often utilized with conductive filling nanomaterials. However, due to the dielectric properties of the polymer and oxide layer in LM, the electrical conductivity hindered practical applications. Saborio *et al.* synthesized a complex with PDMS, LM droplets and graphene flakes to form electrically conductive and continuous pathways within the polymeric matrix.<sup>80</sup> This method minimized the oxidation of the LM droplets which contributed to a high conductivity of  $39.0 \text{ S cm}^{-1}$ , and mechanical durability. Deformable semi-solid particles composed of liquid metal (LMP) have emerged as a prospective alternative to rigid conductive fillers, owing to their commendable electrical characteristics and stable conductivity when subjected to strain. Nonetheless, the attainment of a compact and robust coating for LMP has posed a persistent challenge, primarily attributed to the incompatibility of traditional coating methods with LMP. To address this issue and enhance the uniformity and durability of the LMP coating, carbon nanotubes (CNT) were introduced into the LMP, resulting in the formation of a bi-layer LMP composite-coated fiber characterized by elevated electrical conductivity ( $2.24 \times 10^6 \text{ S m}^{-1}$ ), stretchability, and biocompatibility (Fig. 4g(i)).<sup>81</sup> The bi-layer LMP-coated conductive fiber exhibited stable electrical properties to stretching motions in which the resistance changes were negligible under 10 000 cycles of 150% strains and peel test. By utilizing this fiber, a bi-LMP coated fiber was implanted into sciatic nerve to measure muscular physiology and EMG signal upon electrical stimulation (Fig. 4g(ii)). Liquid-metal-based electronics have solved various issues present in soft electronics as they serve as flexible liquid conductors and

circuits with exceptional electrical conductivity and conformability. However, the mechanical robustness of the oxidation layer and merging issues still require further investigations, taking advantage of composites to improve the mechanical properties.

### 3 Liquid-infused surfaces for encapsulation

Water can result in detrimental damages to soft electronic devices in a form of short-circuiting, corrosion, and degradation, which significantly reduce their performance and reliability.<sup>19,82</sup> Therefore, the importance of encapsulation technology has been highlighted alongside state-of-the-art electronics to prevent water permeation during operation. Mechanical sealing and conformal coatings currently constitute the most common encapsulation methods used to protect electronic devices against water damage. Mechanical sealing approach prevents moisture permeation by forming water-tight encapsulation.<sup>83,84</sup> However, such mechanical sealing increases device size and stiffness, making it unsuitable to be implemented in flexible electronics and potentially leading to delamination of the encapsulation or failure over time. As an alternative, polymeric film-based encapsulation (*e.g.*, epoxy resins, urethane, and silicone gels) provides conformal sealing, which is more flexible and compact. Still, it fails to deliver absolute molecular-scale water protection since the coating processes induce voids and cracks that break the seal, allowing water to permeate.<sup>85,86</sup>

In contrast to conventional encapsulation methods, living organisms have adopted diverse strategies to prevent infiltration of ions and water for their sensitive chemical systems. These strategies typically hinge on the collaborative action of viscous fluids and polymer networks, forming a resilient, flexible, and self-healing outer coating. One living organism that employs the strategy is the waxy monkey tree frog, *Phyllomedusa sauvagii*. To protect its sensitive skin and organs in the hot season, it covers its skin with an oily fluid.<sup>87</sup> The frog can endure extended periods without water as it secretes the oil once again to refill the depleted parts of the skin. Similarly, the human body implements the same strategy to protect stomach lining *via* a coating of mucus, a fluid-infused polymer matrix. The fluid-infused coating layer is resistant against the corrosive acidic environment, also providing a smooth lubricating passage of food intake. This overarching approach of entrapping lubricant within an interface has been implemented to impede water permeation to electronic components while preserving desirable attributes such as mechanical compliance and self-healing properties. Lubricant-infused surface modification was demonstrated by Aizenberg *et al.*<sup>88,89</sup> Inspired by the *Nepenthes* pitcher plant, they fabricated a porous surface and rendered its surface hydrophobic using fluorinated silane. Then, the fluorinated lubricant with matching surface tension with that of the surface became infused to exhibit



outstanding anti-biofouling, transparency, and liquid-repellent characteristics. This novel idea innovated various fields of studies, which include marine science,<sup>90,91</sup> gas transport,<sup>92</sup> water harvesting,<sup>93,94</sup> and medical devices,<sup>95–98</sup> but no studies have applied a slippery lubricant-infused surface as encapsulation material for electronics. Sun *et al.* demonstrated the capability of liquid-infused encapsulation using fluorinated lubricant and roughly patterned silicone elastomer as a substrate (Fig. 5b(i)).<sup>99</sup> Despite the silicone elastomer being known to have high gas permeability, the defect-free nature of the infused oil prevented water permeation through potential cracks, pinholes, or free volume. The diffusion barrier characteristics of the infused liquid were tested *via* magnesium degradation test and water vapor transport test maintaining robust water barrier characteristics for 226 days at body temperature (Fig. 5b(ii) and (iii)). This could be attributed to the defect-free nature and self-healing properties of the lubricant suggesting the potential of the liquid-based encapsulation. However, the surface energy disparity between the silicone elastomer and fluorinated lubricant may have hindered its water barrier characteristics for further operating duration. To further improve the performance of liquid-infused encapsulation, Lemaire *et al.* fabricated a hydrophobic oil-infused polymer matrix (Fig. 5c(i)).<sup>100</sup> To test its water protection abilities, highly water-sensitive optoelectronic materials, methylammonium lead iodide perovskite thin films (MAPbI<sub>3</sub>), were used. The test demonstrated that the encapsulation layer coated with lubricant-infused polymer

significantly reduces water damage, prolonging the perovskite film's lifespan. The underlying mechanism of liquid-infused encapsulation is that the infused hydrophobic oil causes water to form clusters due to small pore sizes within the polymer matrix. Additionally, the infused fluid maintains a defect-free polymer matrix at the molecular level, eliminating low-energy diffusion pathways induced by artifacts or damage. Notably, the lubricant-infused encapsulation layer not only protects electronics from wet environments, but also offers favorable characteristics for bioelectronics, which include transparency, self-healing of the lubricant layer, and anti-biofouling properties. Despite the excellent anti-fouling and encapsulation of the liquid-infused surface, the depletion of the infused liquid may degrade its performances, requiring further investigations.

## 4 Liquid-based adhesives

Current soft electronics require conformable structures with rigid electronic components. The rigid electronic components are commonly composed of various materials like metal interconnectors, silicon, polymers, *etc.*<sup>101</sup> In order to integrate these different materials, commercially available cyanoacrylate-based adhesives and epoxy are usually applied to bond them together.<sup>102–104</sup> The immediate bonding capability and low cost benefit easy fabrication of devices. However, cyanoacrylate-based adhesives become vulnerable to mechanical impact or temperature as they cure, becoming stiff.<sup>105</sup> Moreover, such adhesive does not cure on silicone-

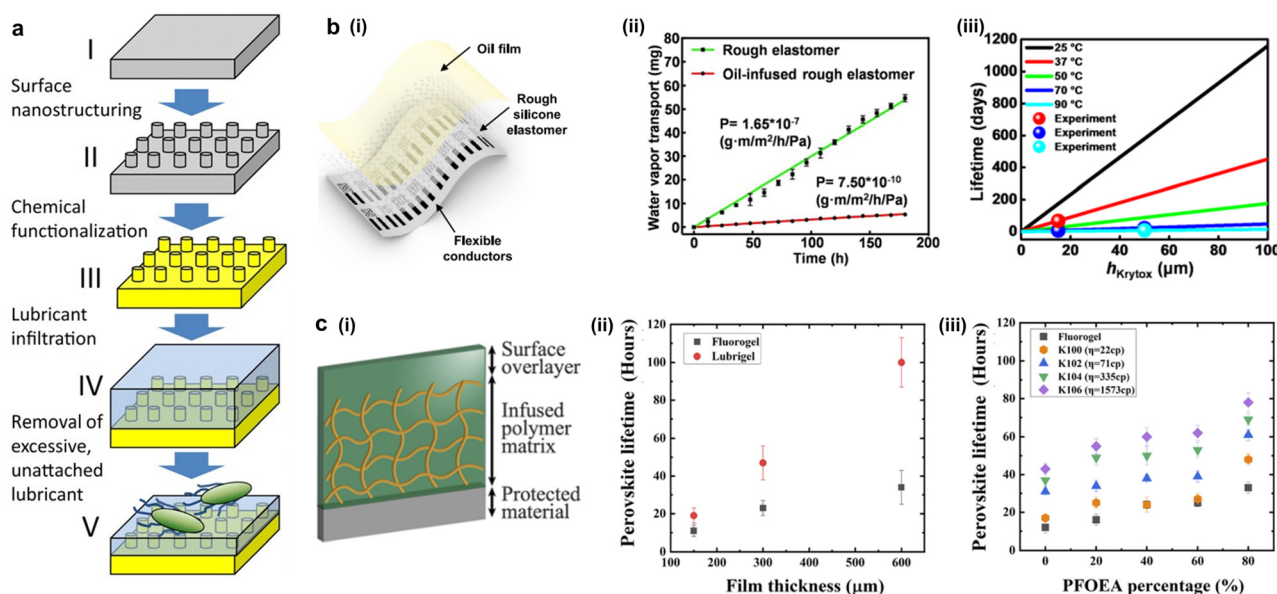


**Fig. 5** Liquid-infused encapsulation. (a) Schematics for fabrication of slippery liquid-infused surface with exceptional anti-biofouling performance (reproduced with permission from ref. 89. Copyright 2012 *National Academy of Sciences*). (b) (i) Schematic illustration of oil-infused rough silicone elastomer. (ii) Water-vapor permeability of rough elastomer versus oil-infused elastomers. (iii) Lifetime changes at different temperatures with the oil thickness (reproduced with permission from ref. 98. Copyright 2021 *American Chemical Society*). (c) (i) Schematic illustration of oil-infused fluorogel matrix. (ii) Performance of fluorogel and oil-infused fluorogel by immersing the protected perovskite films in a water bath. (iii) The lifetime of the perovskite films in a water bath with functions of different PFOEA and different oils (reproduced with permission from ref. 99. Copyright 2023 *National Academy of Sciences*).

based elastomers which are commonly adopted for soft electronic devices as a substrate, making it unfavorable for applications.<sup>106</sup> To overcome these challenges, various researchers have reported hydrogel-based adhesive as a possible candidate to be applied as an interface in soft electronics. A hydrogel-based adhesive possesses favorable characteristics of a liquid, with a modulus comparable to that of tissues, and biocompatibility for soft electronic applications. However, the innate high water contents and low modulus have been known to hinder practical applications. To improve the integrity and adhesive properties of the hydrogels, organic compounds can be used with abundant functional groups to promote crosslinking within the hydrogels, while providing active bonding sites through chemical interactions, allowing non-selective adhesion. As a natural model for adhesives, marine mussels have been highlighted for their ability to strongly adhere to various types of surfaces in dynamic ocean environments. The secreted mussel foot proteins (MFPs) form a byssal thread which exhibits strong interfacial binding to foreign surfaces. This phenomenon is owing to the high contents of catechol, which can form hydrogen bonds and various chemical bonds allowing adhesive capabilities of the mussel. Inspired by the abundant catechol in mussel, Barrett *et al.* reported mechanically robust hydrogel adhesive with controlled swelling and adhesion to soft tissue.<sup>107</sup> The hydrogel is fabricated using a branched amphiphilic PPO-PEO block copolymer that is terminated with catechol. The catechol provided adhesive capabilities to soft surfaces; however, the short-term adhesiveness and limited reusability have been reported as limitations. To achieve long-term adhesiveness, multi-crosslinking of both covalent and non-covalent bonds was promoted to fabricate a mechanically durable hydrogel with interpenetrating polymer networks. Gan *et al.* designed a hydrogel containing Ag-lignin nanoparticles, pectin, and acrylic acid (Fig. 6a).<sup>108</sup> The catechol groups generated by the incorporated nanoparticles enhance the hydrogel adhesive properties allowing stable and repeated adhesion. Fig. 6a(i) demonstrates the adhesion mechanism that enables bonding with various types of foreign surfaces including tissue, metals, and polymers. For the surfaces with amine or thiol functional groups, the bonding can be established through Schiff base or Michael addition processes. Otherwise, non-specific binding can be realized by noncovalent bonding such as hydrogen bonding,  $\pi$ - $\pi$  stacking, and metal coordination or chelating. This versatile bonding mechanism allows the hydrogel to adhere to a spectrum of surfaces, including both hydrophilic and hydrophobic materials such as polypropylene (PP), polytetrafluoroethylene (PTFE), and rubber (Fig. 6a(ii)).

Another natural ingredient commonly used in hydrogel adhesive is chitosan. Chitosan is a prospective material for flexible bioelectronics, due to its excellent biocompatibility, water content, conformability to soft tissues, and bio-adhesiveness.<sup>109,110</sup> Quaternized chitosan (QCS) was used for its biocompatibility, pH responsiveness, and amphipathicity

to fabricate a thermo-responsive hydrogel.<sup>111</sup> The hydrogel matrix was further crosslinked with polyacrylic acid (PAA) chains to form dynamic crosslinked networks (Fig. 6b(i)). The versatile adhesive capability of the QCS-PAA hydrogel (QAAH) is facilitated by its crosslinked networks. This attribute arises from synergetic interactions between PAA and QCS. These interactions involve hydrogen bonding between PAA and various substrates, and hydrophobic interactions between the QCS chains and substrates. Together, these mechanisms contribute to the robust adhesive properties of the QCS-PAA hydrogel (Fig. 6b(ii)).

Gelatin is another ingredient commonly utilized to synthesize hydrogel-based adhesive. Phytic acid (PA), gelatin (Gel), and biocompatible poly(vinyl alcohol) (PVA) were used to create a biocompatible conductive hydrogel (Fig. 6c(i)).<sup>112</sup> The resulting PVA/PA/Gel (PPG) hydrogel demonstrated controllable adhesion mechanism with temperature and could easily be removed with a cool compress while adhering to skin and sensing electrophysiological signals when heated (Fig. 6c(ii)). PPG hydrogel's long-term wearability on skin is further guaranteed by its added benefits of breathability, transparency, and antibacterial activity. Because the PPG hydrogel has a reversible physical bond, recycling the waste produced during production is both economical and environmentally beneficial. For electrophysiological signal recording, the PPG hydrogel sensor is a promising candidate adhesive due to its wearability, robust adhesion, and biocompatibility. Jiang *et al.* fabricated hydrogels based on adipic dihydrazide-grafted carboxyethyl chitin (CECT-ADH), dodecyl-grafted carboxyethyl chitosan (CES-DOD), and benzaldehyde-grafted carboxyethyl poly(vinyl alcohol) (PVA-BA).<sup>113</sup> Notably, the hydrogels incorporate multiple dynamic bonds in the polymer network, imparting strength to the hydrogels and creating an extracellular matrix (ECM)-mimetic microenvironment. This allows a compatible environment that promotes the differentiation of rat bone mesenchymal stem cells (rBMSC). The hydrogels mimicking the ECM microenvironment demonstrate outstanding biocompatibility, supporting intricate cellular function, but also inherent adhesion capability to various tissue surfaces. The remarkable properties of these dynamic hydrogel adhesives were thoroughly assessed *in vivo*. Zhang *et al.* reported an ionic conductive hydrogel based on polyacrylamide and gelatin for sensing movements and harvesting body heat.<sup>114</sup> The hydrogel demonstrates robust mechanical properties, including an elongation of 1424% and a tensile stress of 129.1 kPa at room temperature. For the detachment of the hydrogel, it loses its adhesion when it is chilled by an ice bag. The hydrogel, when assembled into a thermoelectric generator, is employed to harness body heat, and convert it into electricity for power supply. Another study reported a hydrogel powder based on polyethyleneimine/polyacrylic acid/quaternized chitosan (PEI/PAA/QCS) with rapid hemostatic and adhesive properties. The powder exhibited self-gelling behavior upon absorption of anti-coagulated blood (Fig. 6d(i)).<sup>115</sup> For practical application, this powder can be deposited on a bleeding site to absorb the blood, forming an adhesive hydrogel *in situ* within four seconds





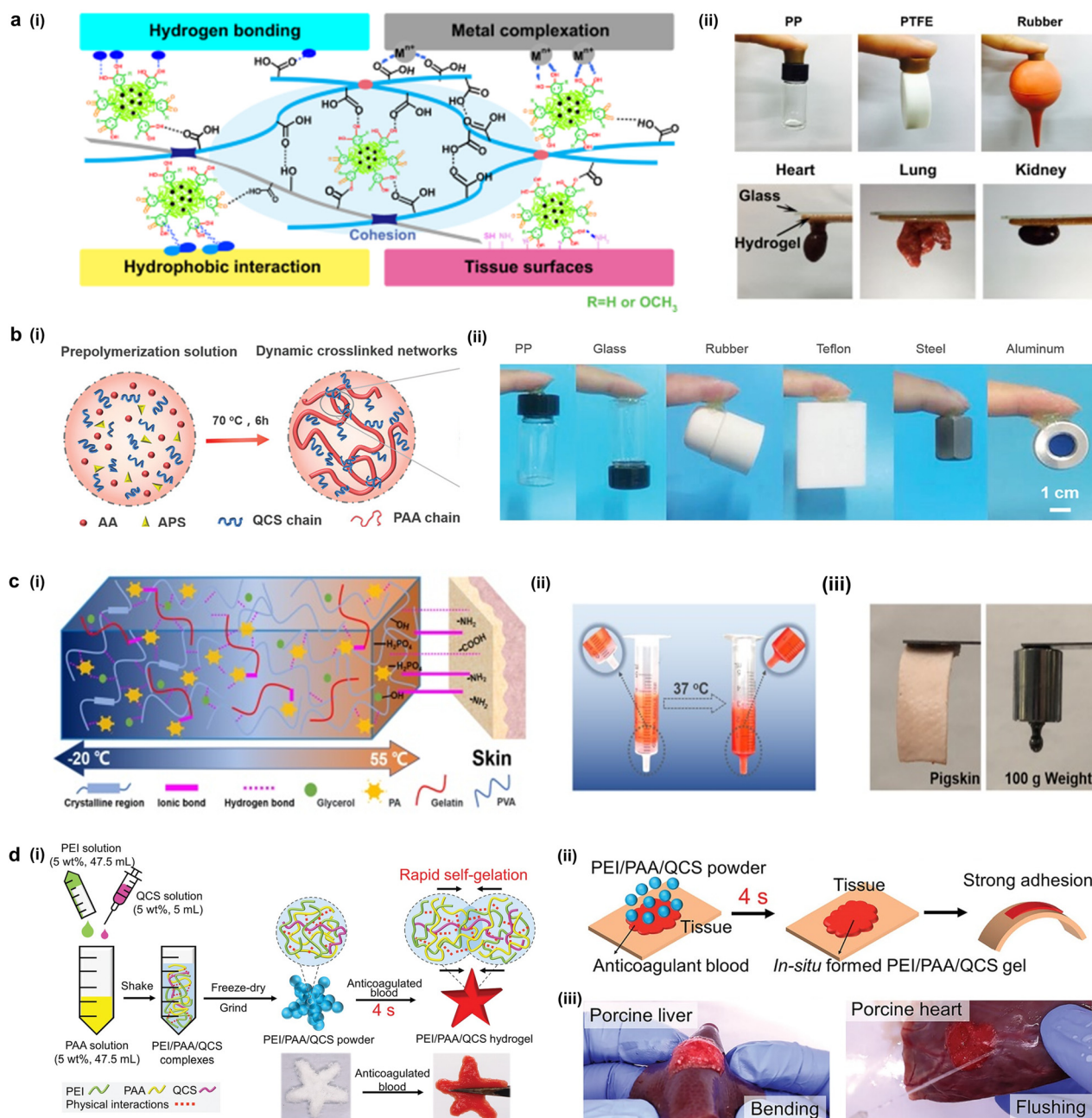


**Fig. 6** Liquid-based adhesive. (a) (i) Schematic illustration of the adhesion mechanism of catechol-based NPs-P-PAA hydrogel. (ii) Adhesive property of the hydrogel to diverse solids and skin surfaces (reproduced from ref. 108. Copyright 2019 *Springer Nature*). (b) (i) Scheme of the preparation process of ionic conductive hydrogel. (ii) Adhesive property to various polymers and metal substrates (reproduced from ref. 111. Copyright 2021 *John Wiley and Sons*). (c) (i) Schematic illustration of the mechanism of controllable adhesion of PPG hydrogel. (ii) Self-adaptive property of PPF hydrogel marked with Rh B at 37 °C. (iii) Self-adhesion property of PPG hydrogel to porcine skin and 100 g weight (reproduced from ref. 112. Copyright 2022 *Springer Nature*). (d) (i) Schematic illustrations for the preparation of PEI/PAA/QCS powder and the formation of PEI/PAA/QCS powder-derived hydrogel by adding anticoagulated blood. (ii) Schematic illustration of the robust adhesion mechanism of PEI/PAA/QCS powder. (iii) Photos of the robust bioadhesion of PEI/PAA/QCS powder on porcine liver and heart (reproduced from ref. 115. Copyright 2021 *Advanced Functional Materials*).

(Fig. 6d(ii)). The hydrogel stops further bleeding from the wound site, while improving wound healing efficiency owing to its firm adhesion and hemostatic capability. Notably, the application of PEI/PAA/QCS powder was demonstrated to be effective in sealing damaged mouse liver, heart, femoral artery and tail vein (Fig. 6d(iii)). The notable features of this powder

include robust wet adhesion, excellent cytocompatibility, adaptability to conform to complex tissue surfaces, and a simple synthesis process, rendering it a promising bioadhesive for a myriad of biomedical applications. Despite the advancements in liquid-based adhesives, future investigations are required to overcome selective adhesion and enhance mechanical stability.



**Table 1** Liquid-based electronic materials and their performance

	Material	Elongation (%)	Conductivity	Durability (number of cycles)	Application	Ref.
Ionic hydrogel	Polyacrylamide-NaCl	500	—	1000	Strain sensor	30
	Ionic PDMS	539.1	0.25 mS m <sup>-1</sup>	1000	Grid-less touch sensor	41
	PVA/borax/sodium tetraborate	700	2.9 × 10 <sup>-5</sup> S cm <sup>-1</sup>	500	Wearable energy harvesting device	40
Nanomaterial-incorporated conductive hydrogel	PAAM-alginate-Ag flake	250	374 S cm <sup>-1</sup>	1000	Neuromuscular electrical stimulation electrode	50
	Silk fibroin-rGO-CaCl <sub>2</sub>	1500	1 × 10 <sup>-2</sup> S cm <sup>-1</sup>	4	Bionic glove	53
	PVA-TA-PAA-CNT	1000	40 S m <sup>-1</sup>	1000	EMG/strain sensing	57, 58
Liquid metal	Mxene-doped liquid metal	>200	2.20 × 10 <sup>6</sup> S m <sup>-1</sup>	2000	Temperature sensor	69
	CNT-attached liquid metal particles	150	2.24 × 10 <sup>6</sup> S m <sup>-1</sup>	10 000	Neural recording and stimulation	79
	PDMS-graphene-liquid metal	80	39 S cm <sup>-1</sup>	—	Flexible conductor	80
	Liquid metal-silicone	300	3.4 × 10 <sup>6</sup> S m <sup>-1</sup>	10 000	Monitoring artery pulse	81

## 5 Conclusions

In this review, we introduced known limitations present in current solid-state electronics regarding their mechanical disparities and biological compatibility for applications in soft electronics, and demonstrated recent work that overcomes the hurdles. The liquid-based materials provide inherent flexibility and conformability, which reduce the mechanical mismatch between human tissues and devices and greatly improve devices' usability. By adopting liquid-based materials that are intrinsically soft and conformal, it could narrow the mechanical gap between soft tissues and electronics. As a component of soft electronics, liquid-based conductors were introduced using ionic liquids, liquid metals, and nanomaterial-incorporated hydrogels (Table 1). Compared to solid electronic materials, these soft electronic materials could provide versatile functionalities owing to their degree of freedom in their compositions which immensely improves their mechanical durability and applicability in practical applications. Moreover, recent innovations in soft electronics allowed fabrication of soft electronic materials with high durability and flexibility. Another important aspect is innovation in defect-free encapsulation. Despite rapid development of electronics, the encapsulation technology still falls behind, limiting the practical applications of electronic devices. The liquid-infused encapsulation technology could minimize device performance degradation by reducing the defects within the polymer structures and preventing water permeation. Moreover, anti-biofouling properties of encapsulation could provide long-term stability especially in implantable soft electronics. Furthermore, nature-inspired adhesive materials allow stable and conformal adhesion of solid electronic materials to moist, irregular, and dynamic tissue surfaces. To conclude, we believe that liquid-based materials in soft electronics have started a first stage to the implementation of practical applications. These liquid-based materials exhibit 1) superior conformality, 2) biocompatibility, 3)

flexibility, 4) mechanical durability, and 5) adaptability to versatile applications without compromising electrical conductivity. Therefore, further investigations are required to utilize the full potential of these liquid-based materials. For example, current developments of state-of-the-art soft electronic devices cannot be advanced without using solid-based electronics due to their stability and functionalities. However, further research in liquid-based electronic materials could realize soft electronic devices with liquid-based conductors, encapsulation, and adhesives to achieve all-soft electronic devices. Lastly, soft electronic devices that could be seamlessly integrated to the human body are poised to bridge the gap between humans and machines. Thereby, highly sophisticated human-machine interfaces could be achieved, advancing healthcare management systems.

## Conflicts of interest

The authors declare no conflicts of interest.

## Acknowledgements

This work was supported by the National Research Foundation of Korea (NRF) funded by Ministry of Science and ICT (project numbers: 2022M3E5E9082213; NRF-2022R1A2C4001652). This work was supported by the Korea Medical Device Development Fund grant funded by the Korea government (Ministry of Science and ICT, Ministry of Trade, Industry and Energy, Ministry of Health & Welfare, Ministry of Food and Drug Safety) (project number: RS-2023-00243310).

## References

- 1 S. H. Byun, J. Y. Sim, K. C. Agno and J. W. Jeong, Materials and manufacturing strategies for mechanically transformative electronics, *Mater. Today Adv.*, 2020, 7, 100089.



- 2 S. Liu, Y. Rao, H. Jang, P. Tan and N. Lu, Strategies for body-conformable electronics, *Matter*, 2022, **5**, 1104–1136.
- 3 W. Gao, J. Huang, J. He, R. Zhou, Z. Li, Z. Chen, Y. Zhang and C. Pan, Recent advances in ultrathin materials and their applications in e-skin, *InfoMat*, 2023, **5**, e12426.
- 4 Z. Xue, H. Song, J. A. Rogers, Y. Zhang and Y. Huang, Mechanically-Guided Structural Designs in Stretchable Inorganic Electronics, *Adv. Mater.*, 2020, **32**, 1902254.
- 5 K. W. Cho, S.-H. Sunwoo, Y. J. Hong, J. H. Koo, J. H. Kim, S. Baik, T. Hyeon and D.-H. Kim, Soft Bioelectronics Based on Nanomaterials, *Chem. Rev.*, 2022, **122**, 5068–5143.
- 6 D.-H. Kim, R. Ghaffari, N. Lu and J. A. Rogers, Flexible and Stretchable Electronics for Biointegrated Devices, *Annu. Rev. Biomed. Eng.*, 2012, **14**, 113–128.
- 7 J.-K. Song, K. Do, J. H. Koo, D. Son and D.-H. Kim, Nanomaterials-based flexible and stretchable bioelectronics, *MRS Bull.*, 2019, **44**, 643–656.
- 8 Y. R. Jeong, G. Lee, H. Park and J. S. Ha, Stretchable, skin-attachable electronics with integrated energy storage devices for biosignal monitoring, *Acc. Chem. Res.*, 2018, **52**, 91–99.
- 9 W. B. Han, G.-J. Ko, T.-M. Jang and S.-W. Hwang, Materials, devices, and applications for wearable and implantable electronics, *ACS Appl. Electron. Mater.*, 2021, **3**, 485–503.
- 10 A. Chortos, J. Liu and Z. Bao, Pursuing prosthetic electronic skin, *Nat. Mater.*, 2016, **15**, 937–950.
- 11 A. J. Bandodkar, P. Gutruf, J. Choi, K. Lee, Y. Sekine, J. T. Reeder, W. J. Jeang, A. J. Aranyosi, S. P. Lee, J. B. Model, R. Ghaffari, C.-J. Su, J. P. Leshock, T. Ray, A. Verrillo, K. Thomas, V. Krishnamurthi, S. Han, J. Kim, S. Krishnan, T. Hang and J. A. Rogers, Battery-free, skin-interfaced microfluidic/electronic systems for simultaneous electrochemical, colorimetric, and volumetric analysis of sweat, *Sci. Adv.*, 2019, **5**, eaav3294.
- 12 S. Wang, Y. Fang, H. He, L. Zhang, C. A. Li and J. Ouyang, Wearable Stretchable Dry and Self-Adhesive Strain Sensors with Conformal Contact to Skin for High-Quality Motion Monitoring, *Adv. Funct. Mater.*, 2021, **31**, 2007495.
- 13 J. W. Salatino, K. A. Ludwig, T. D. Y. Kozai and E. K. Purcell, Glial responses to implanted electrodes in the brain, *Nat. Biomed. Eng.*, 2017, **1**, 862–877.
- 14 S. Gong, L. W. Yap, B. Zhu and W. Cheng, Multiscale soft-hard interface design for flexible hybrid electronics, *Adv. Mater.*, 2020, **32**, 1902278.
- 15 Y. Li, N. Li, W. Liu, A. Prominski, S. Kang, Y. Dai, Y. Liu, H. Hu, S. Wai and S. Dai, Achieving tissue-level softness on stretchable electronics through a generalizable soft interlayer design, *Nat. Commun.*, 2023, **14**, 4488.
- 16 R. Feiner and T. Dvir, Tissue–electronics interfaces: from implantable devices to engineered tissues, *Nat. Rev. Mater.*, 2017, **3**, 17076.
- 17 R. Herbert, J.-H. Kim, Y. S. Kim, H. M. Lee and W.-H. Yeo, Soft Material-Enabled, Flexible Hybrid Electronics for Medicine, Healthcare, and Human-Machine Interfaces, *Materials*, 2018, **11**, 187.
- 18 H.-R. Lim, H. S. Kim, R. Qazi, Y.-T. Kwon, J.-W. Jeong and W.-H. Yeo, Advanced Soft Materials, Sensor Integrations, and Applications of Wearable Flexible Hybrid Electronics in Healthcare, Energy, and Environment, *Adv. Mater.*, 2020, **32**, 1901924.
- 19 İ. Baylakoğlu, A. Fortier, S. Kyeong, R. Ambat, H. Conseil-Gudla, M. H. Azarian and M. G. Pecht, The detrimental effects of water on electronic devices, *e-Prime - Advances in Electrical Engineering, Electronics and Energy*, 2021, **1**, 100016.
- 20 A. Stacy, M. Gilaki, E. Sahraei and D. Soudbakhsh, Investigating the Effects of Mechanical Damage on Electrical Response of Li-Ion Pouch Cells, *2020 American Control Conference (ACC)*, 2020.
- 21 Y. Zhao, A. Kim, G. Wan and B. C. K. Tee, Design and applications of stretchable and self-healable conductors for soft electronics, *Nano Convergence*, 2019, **6**, 25.
- 22 J. A. Fan, W.-H. Yeo, Y. Su, Y. Hattori, W. Lee, S.-Y. Jung, Y. Zhang, Z. Liu, H. Cheng, L. Falgout, M. Bajema, T. Coleman, D. Gregoire, R. J. Larsen, Y. Huang and J. A. Rogers, Fractal design concepts for stretchable electronics, *Nat. Commun.*, 2014, **5**, 3266.
- 23 N. Bowden, S. Brittain, A. G. Evans, J. W. Hutchinson and G. M. Whitesides, Spontaneous formation of ordered structures in thin films of metals supported on an elastomeric polymer, *Nature*, 1998, **393**, 146–149.
- 24 W. Wu, L. Li, Z. Li, J. Sun and L. Wang, Extensible Integrated System for Real-Time Monitoring of Cardiovascular Physiological Signals and Limb Health, *Adv. Mater.*, 2023, **35**, 2304596.
- 25 J. Hubertus, J. Neu, S. Croce, G. Rizzello, S. Seelecke and G. Schultes, Nanoscale Nickel-Based Thin Films as Highly Conductive Electrodes for Dielectric Elastomer Applications with Extremely High Stretchability up to 200%, *ACS Appl. Mater. Interfaces*, 2021, **13**, 39894–39904.
- 26 Y. Chan, M. Skreta, H. McPhee, S. Saha, R. Deus and L. Soleymani, Solution-processed wrinkled electrodes enable the development of stretchable electrochemical biosensors, *Analyst*, 2019, **144**, 172–179.
- 27 Y. Zhang and X. Hou, Liquid-based materials, *National Science Open*, 2022, **1**, 20220035.
- 28 Y. Cao, Y. J. Tan, S. Li, W. W. Lee, H. Guo, Y. Cai, C. Wang and B. C. K. Tee, Self-healing electronic skins for aquatic environments, *Nat. Electron.*, 2019, **2**, 75–82.
- 29 H.-R. Lee, C.-C. Kim and J.-Y. Sun, Stretchable Ionics – A Promising Candidate for Upcoming Wearable Devices, *Adv. Mater.*, 2018, **30**, 1704403.
- 30 J.-Y. Sun, C. Keplinger, G. M. Whitesides and Z. Suo, Ionic skin, *Adv. Mater.*, 2014, **26**, 7608–7614.
- 31 Y. Cao, T. G. Morrissey, E. Acome, S. I. Allec, B. M. Wong, C. Keplinger and C. Wang, A Transparent, Self-Healing, Highly Stretchable Ionic Conductor, *Adv. Mater.*, 2017, **29**, 1605099.
- 32 Y. Wu, Y. Zhou, W. Asghar, Y. Liu, F. Li, D. Sun, C. Hu, Z. Wu, J. Shang, Z. Yu, R.-W. Li and H. Yang, Liquid Metal-Based Strain Sensor with Ultralow Detection Limit for Human–Machine Interface Applications, *Advanced Intelligent Systems*, 2021, **3**, 2000235.





- 33 J. Park, Y. Lee, T. Y. Kim, S. Hwang and J. Seo, Functional Bioelectronic Materials for Long-Term Biocompatibility and Functionality, *ACS Appl. Electron. Mater.*, 2022, **4**, 1449–1468.
- 34 Y. Liu, J. Liu, S. Chen, T. Lei, Y. Kim, S. Niu, H. Wang, X. Wang, A. M. Foudeh, J. B. H. Tok and Z. Bao, Soft and elastic hydrogel-based microelectronics for localized low-voltage neuromodulation, *Nat. Biomed. Eng.*, 2019, **3**, 58–68.
- 35 V. R. Feig, H. Tran, M. Lee and Z. Bao, Mechanically tunable conductive interpenetrating network hydrogels that mimic the elastic moduli of biological tissue, *Nat. Commun.*, 2018, **9**, 2740.
- 36 Q. Gui, Y. He and Y. Wang, Soft Electronics Based on Liquid Conductors, *Adv. Electron. Mater.*, 2021, **7**, 2000780.
- 37 L. Guan, A. Nilghaz, B. Su, L. Jiang, W. Cheng and W. Shen, Stretchable-Fiber-Confined Wetting Conductive Liquids as Wearable Human Health Monitors, *Adv. Funct. Mater.*, 2016, **26**, 4511–4517.
- 38 R. Tong, Z. Ma, P. Gu, R. Yao, T. Li, M. Zeng, F. Guo, L. Liu and J. Xu, Stretchable and sensitive sodium alginate ionic hydrogel fibers for flexible strain sensors, *Int. J. Biol. Macromol.*, 2023, **246**, 125683.
- 39 S. H. Cho, S. W. Lee, S. Yu, H. Kim, S. Chang, D. Kang, I. Hwang, H. S. Kang, B. Jeong, E. H. Kim, S. M. Cho, K. L. Kim, H. Lee, W. Shim and C. Park, Micropatterned Pyramidal Ionic Gels for Sensing Broad-Range Pressures with High Sensitivity, *ACS Appl. Mater. Interfaces*, 2017, **9**, 10128–10135.
- 40 K. Parida, V. Kumar, W. Jiangxin, V. Bhavanasi, R. Bendi and P. S. Lee, Highly Transparent, Stretchable, and Self-Healing Ionic-Skin Triboelectric Nanogenerators for Energy Harvesting and Touch Applications, *Adv. Mater.*, 2017, **29**, 1702181.
- 41 Y. Lee, S. Lim, W. J. Song, S. Lee, S. J. Yoon, J.-M. Park, M.-G. Lee, Y.-L. Park and J.-Y. Sun, Triboresistive Touch Sensing: Grid-Free Touch-Point Recognition Based on Monolayered Ionic Power Generators, *Adv. Mater.*, 2022, **34**, 2108586.
- 42 V. R. Feig, H. Tran, M. Lee, K. Liu, Z. Huang, L. Beker, D. G. Mackanic and Z. Bao, An Electrochemical Gelation Method for Patterning Conductive PEDOT:PSS Hydrogels, *Adv. Mater.*, 2019, **31**, e1902869.
- 43 J. Deng, H. Yuk, J. Wu, C. E. Varela, X. Chen, E. T. Roche, C. F. Guo and X. Zhao, Electrical bioadhesive interface for bioelectronics, *Nat. Mater.*, 2021, **20**, 229–236.
- 44 W. Huang, Y. Zhang, Q. You, P. Huang, Y. Wang, Z. N. Huang, Y. Ge, L. Wu, Z. Dong, X. Dai, Y. Xiang, J. Li, X. Zhang and H. Zhang, Enhanced Photodetection Properties of Tellurium@Selenium Roll-to-Roll Nanotube Heterojunctions, *Small*, 2019, **15**, 1900902.
- 45 H. Pan, H. Chu, Y. Li, Z. Pan, J. Zhao, S. Zhao, W. Huang and D. Li, Bismuthene quantum dots integrated D-shaped fiber as saturable absorber for multi-type soliton fiber lasers, *J. Mater.*, 2023, **9**, 183–190.
- 46 W. Huang, J. Zhu, M. Wang, L. Hu, Y. Tang, Y. Shu, Z. Xie and H. Zhang, Emerging Mono-Elemental Bismuth Nanostructures: Controlled Synthesis and Their Versatile Applications, *Adv. Funct. Mater.*, 2021, **31**, 2007584.
- 47 Y. Zi, Y. Hu, J. Pu, M. Wang and W. Huang, Recent Progress in Interface Engineering of Nanostructures for Photoelectrochemical Energy Harvesting Applications, *Small*, 2023, **19**, 2208274.
- 48 Y. Zi, J. Zhu, M. Wang, L. Hu, Y. Hu, S. Wageh, O. A. Al-Hartomy, A. Al-Ghamdi, W. Huang and H. Zhang, CdS@CdSe Core/Shell Quantum Dots for Highly Improved Self-Powered Photodetection Performance, *Inorg. Chem.*, 2021, **60**, 18608–18613.
- 49 H. Xu, Y. Lv, D. Qiu, Y. Zhou, H. Zeng and Y. Chu, An ultra-stretchable, highly sensitive and biocompatible capacitive strain sensor from an ionic nanocomposite for on-skin monitoring, *Nanoscale*, 2019, **11**, 1570–1578.
- 50 Y. Ohm, C. Pan, M. J. Ford, X. Huang, J. Liao and C. Majidi, An electrically conductive silver–polyacrylamide–alginate hydrogel composite for soft electronics, *Nat. Electron.*, 2021, **4**, 185–192.
- 51 Y. Liu, X. Shi, S. Liu, H. Li, H. Zhang, C. Wang, J. Liang and Y. Chen, Biomimetic printable nanocomposite for healable, ultrasensitive, stretchable and ultradurable strain sensor, *Nano Energy*, 2019, **63**, 103898.
- 52 J. Lv, C. Kong, C. Yang, L. Yin, I. Jeerapan, F. Pu, X. Zhang, S. Yang and Z. Yang, Wearable, stable, highly sensitive hydrogel–graphene strain sensors, *Beilstein J. Nanotechnol.*, 2019, **10**, 475–480.
- 53 F. B. Kadumudi, M. Hasany, M. K. Pierchala, M. Jahanshahi, N. Taebnia, M. Mehrali, C. F. Mitu, M.-A. Shahbazi, T.-G. Zsurzsan, A. Knott, T. L. Andresen and A. Dolatshahi-Pirouz, The Manufacture of Unbreakable Bionics via Multifunctional and Self-Healing Silk–Graphene Hydrogels, *Adv. Mater.*, 2021, **33**, 2100047.
- 54 M. Atif, I. Afzaal, H. Naseer, M. Abrar and R. Bongiovanni, Review—Surface Modification of Carbon Nanotubes: A Tool to Control Electrochemical Performance, *ECS J. Solid State Sci. Technol.*, 2020, **9**, 041009.
- 55 S. Xia, S. Song, F. Jia and G. Gao, A flexible, adhesive and self-healable hydrogel-based wearable strain sensor for human motion and physiological signal monitoring, *J. Mater. Chem. B*, 2019, **7**, 4638–4648.
- 56 L. Han, K. Liu, M. Wang, K. Wang, L. Fang, H. Chen, J. Zhou and X. Lu, Mussel-Inspired Adhesive and Conductive Hydrogel with Long-Lasting Moisture and Extreme Temperature Tolerance, *Adv. Funct. Mater.*, 2018, **28**, 1704195.
- 57 J. Park, J. Y. Kim, J. H. Heo, Y. Kim, S. A. Kim, K. Park, Y. Lee, Y. Jin, S. R. Shin, D. W. Kim and J. Seo, Intrinsically Nonswellable Multifunctional Hydrogel with Dynamic Nanoconfinement Networks for Robust Tissue-Adaptable Bioelectronics, *Adv. Sci.*, 2023, **10**, 2207237.
- 58 S. A. Kim, Y. Lee, K. Park, J. Park, S. An, J. Oh, M. Kang, Y. Lee, Y. Jo, S. W. Cho and J. Seo, 3D printing of mechanically tough and self-healing hydrogels with carbon nanotube fillers, *Int. J. Bioprint.*, 2023, **9**, 765.
- 59 J. He, S. Liang, F. Li, Q. Yang, M. Huang, Y. He, X. Fan and M. Wu, Recent Development in Liquid Metal Materials, *ChemistryOpen*, 2021, **10**, 360–372.



- 60 L. Gu, S. Poddar, Y. Lin, Z. Long, D. Zhang, Q. Zhang, L. Shu, X. Qiu, M. Kam, A. Javey and Z. Fan, A biomimetic eye with a hemispherical perovskite nanowire array retina, *Nature*, 2020, **581**, 278–282.
- 61 G. Yun, S.-Y. Tang, S. Sun, D. Yuan, Q. Zhao, L. Deng, S. Yan, H. Du, M. D. Dickey and W. Li, Liquid metal-filled magnetorheological elastomer with positive piezoconductivity, *Nat. Commun.*, 2019, **10**, 1300.
- 62 M. D. Dickey, Stretchable and Soft Electronics using Liquid Metals, *Adv. Mater.*, 2017, **29**, 1606425.
- 63 H. Chang, P. Zhang, R. Guo, Y. Cui, Y. Hou, Z. Sun and W. Rao, Recoverable Liquid Metal Paste with Reversible Rheological Characteristic for Electronics Printing, *ACS Appl. Mater. Interfaces*, 2020, **12**, 14125–14135.
- 64 P. Won, C. S. Valentine, M. Zadan, C. Pan, M. Vinciguerra, D. K. Patel, S. H. Ko, L. M. Walker and C. Majidi, 3D Printing of Liquid Metal Embedded Elastomers for Soft Thermal and Electrical Materials, *ACS Appl. Mater. Interfaces*, 2022, **14**, 55028–55038.
- 65 C. Ladd, J.-H. So, J. Muth and M. D. Dickey, 3D Printing of Free Standing Liquid Metal Microstructures, *Adv. Mater.*, 2013, **25**, 5081–5085.
- 66 R. Xing, J. Yang, D. Zhang, W. Gong, T. V. Neumann, M. Wang, R. Huang, J. Kong, W. Qi and M. D. Dickey, Metallic gels for conductive 3D and 4D printing, *Matter*, 2023, **6**, 2248–2262.
- 67 F.-M. Allieux, J. Han, J. Tang, S. Merhebi, S. Cai, J. Tang, R. Abbasi, F. Centurion, M. Mousavi, C. Zhang, W. Xie, M. Mayyas, M. A. Rahim, M. B. Ghasemian and K. Kalantar-Zadeh, Nanotip Formation from Liquid Metals for Soft Electronic Junctions, *ACS Appl. Mater. Interfaces*, 2021, **13**, 43247–43257.
- 68 Q. Wu, F. Zhu, Z. Wu, Y. Xie, J. Qian, J. Yin and H. Yang, Suspension printing of liquid metal in yield-stress fluid for resilient 3D constructs with electromagnetic functions, *npj Flexible Electron.*, 2022, **6**, 50.
- 69 Y. Wu, Y. Li, Y. Zou, W. Rao, Y. Gai, J. Xue, L. Wu, X. Qu, Y. Liu, G. Xu, L. Xu, Z. Liu and Z. Li, A multi-mode triboelectric nanogenerator for energy harvesting and biomedical monitoring, *Nano Energy*, 2022, **92**, 106715.
- 70 Y. Gao, H. Ota, E. W. Schaler, K. Chen, A. Zhao, W. Gao, H. M. Fahad, Y. Leng, A. Zheng, F. Xiong, C. Zhang, L. C. Tai, P. Zhao, R. S. Fearing and A. Javey, Wearable Microfluidic Diaphragm Pressure Sensor for Health and Tactile Touch Monitoring, *Adv. Mater.*, 2017, **29**, 1701985.
- 71 M. D. Dickey, R. C. Chiechi, R. J. Larsen, E. A. Weiss, D. A. Weitz and G. M. Whitesides, Eutectic Gallium-Indium (EGaIn): A Liquid Metal Alloy for the Formation of Stable Structures in Microchannels at Room Temperature, *Adv. Funct. Mater.*, 2008, **18**, 1097–1104.
- 72 Y. R. Jeong, J. Kim, Z. Xie, Y. Xue, S. M. Won, G. Lee, S. W. Jin, S. Y. Hong, X. Feng, Y. Huang, J. A. Rogers and J. S. Ha, A skin-attachable, stretchable integrated system based on liquid GaInSn for wireless human motion monitoring with multi-site sensing capabilities, *NPG Asia Mater.*, 2017, **9**, e443–e443.
- 73 S. Handschuh-Wang, T. Gan, T. Wang, F. J. Stadler and X. Zhou, Surface Tension of the Oxide Skin of Gallium-Based Liquid Metals, *Langmuir*, 2021, **37**, 9017–9025.
- 74 G.-H. Lee, Y. R. Lee, H. Kim, D. A. Kwon, H. Kim, C. Yang, S. Q. Choi, S. Park, J.-W. Jeong and S. Park, Rapid meniscus-guided printing of stable semi-solid-state liquid metal microgranular-particle for soft electronics, *Nat. Commun.*, 2022, **13**, 2643.
- 75 R. Abbasi, M. Mayyas, M. B. Ghasemian, F. Centurion, J. Yang, M. Saborio, F.-M. Allieux, J. Han, J. Tang, M. J. Christoe, K. M. Mohibul Kabir, K. Kalantar-Zadeh and M. A. Rahim, Photolithography-enabled direct patterning of liquid metals, *J. Mater. Chem. C*, 2020, **8**, 7805–7811.
- 76 L. Johnston, J. Yang, J. Han, K. Kalantar-Zadeh and J. Tang, Intermetallic wetting enabled high resolution liquid metal patterning for 3D and flexible electronics, *J. Mater. Chem. C*, 2022, **10**, 921–931.
- 77 M. Baharfar, M. Mayyas, M. Rahbar, F.-M. Allieux, J. Tang, Y. Wang, Z. Cao, F. Centurion, R. Jalili, G. Liu and K. Kalantar-Zadeh, Exploring Interfacial Graphene Oxide Reduction by Liquid Metals: Application in Selective Biosensing, *ACS Nano*, 2021, **15**, 19661–19671.
- 78 Y. Wang, S. Wang, H. Chang and W. Rao, Galvanic Replacement of Liquid Metal/Reduced Graphene Oxide Frameworks, *Adv. Mater. Interfaces*, 2020, **7**, 2000626.
- 79 G.-H. Lee, D. H. Lee, W. Jeon, J. Yoon, K. Ahn, K. S. Nam, M. Kim, J. K. Kim, Y. H. Koo, J. Joo, W. Jung, J. Lee, J. Nam, S. Park, J.-W. Jeong and S. Park, Conductance stable and mechanically durable bi-layer EGaIn composite-coated stretchable fiber for 1D bioelectronics, *Nat. Commun.*, 2023, **14**, 4173.
- 80 M. G. Saborio, S. Cai, J. Tang, M. B. Ghasemian, M. Mayyas, J. Han, M. J. Christoe, S. Peng, P. Koshy, D. Esrafilzadeh, R. Jalili, C. H. Wang and K. Kalantar-Zadeh, Liquid Metal Droplet and Graphene Co-Fillers for Electrically Conductive Flexible Composites, *Small*, 2020, **16**, 1903753.
- 81 M. Li, D. Chen, X. Deng, B. Xu, M. Li, H. Liang, M. Wang, G. Song, T. Zhang and Y. Liu, Graded Mxene-Doped Liquid Metal as Adhesion Interface Aiming for Conductivity Enhancement of Hybrid Rigid-Soft Interconnection, *ACS Appl. Mater. Interfaces*, 2023, **15**, 14948–14957.
- 82 Y.-N. Z. Yip, Z. Zhu and Y.-C. Chan, Reliability of wearable electronics – Case of water proof tests on smartwatch, *2017 IEEE 19th Electronics Packaging Technology Conference (EPTC)*, Singapore, 2017, pp. 1–5.
- 83 D.-S. Kim, Y. W. Choi, A. Shanmugasundaram, Y.-J. Jeong, J. Park, N.-E. Oyunbaatar, E.-S. Kim, M. Choi and D.-W. Lee, Highly durable crack sensor integrated with silicone rubber cantilever for measuring cardiac contractility, *Nat. Commun.*, 2020, **11**, 535.
- 84 K. Li, X. Cheng, F. Zhu, L. Li, Z. Xie, H. Luan, Z. Wang, Z. Ji, H. Wang, F. Liu, Y. Xue, C. Jiang, X. Feng, L. Li, J. A. Rogers, Y. Huang and Y. Zhang, A Generic Soft Encapsulation Strategy for Stretchable Electronics, *Adv. Funct. Mater.*, 2019, **29**, 1806630.



- 85 P. Lall, K. Dornala, J. Suhling, J. Deep and R. Lowe, Fatigue Delamination Crack Growth of Potting Compounds in PCB/Epoxy Interfaces Under Flexure Loading, *ASME 2019 International Technical Conference and Exhibition on Packaging and Integration of Electronic and Photonic Microsystems*, 2019.
- 86 R. Wen, J. Huo, J. Lv, Z. Liu and Y. Yu, Effect of silicone resin modification on the performance of epoxy materials for LED encapsulation, *J. Mater. Sci.: Mater. Electron.*, 2017, **28**, 14522–14535.
- 87 L. A. Blaylock, R. Ruibal and K. Platt-Aloia, Skin structure and wiping behavior of phyllomedusine frogs, *Copeia*, 1976, 283–295.
- 88 T.-S. Wong, S. H. Kang, S. K. Tang, E. J. Smythe, B. D. Hatton, A. Grinthal and J. Aizenberg, Bioinspired self-repairing slippery surfaces with pressure-stable omniphobicity, *Nature*, 2011, **477**, 443–447.
- 89 A. K. Epstein, T.-S. Wong, R. A. Belisle, E. M. Boggs and J. Aizenberg, Liquid-infused structured surfaces with exceptional anti-biofouling performance, *Proc. Natl. Acad. Sci.*, 2012, **109**, 13182–13187.
- 90 S. Kolle, O. Ahanotu, A. Meeks, S. Stafslie, M. Kreder, L. Vanderwal, L. Cohen, G. Waltz, C. S. Lim, D. Slocum, E. M. Greene, K. Hunsucker, G. Swain, D. Wendt, S. L.-M. Teo and J. Aizenberg, On the mechanism of marine fouling-prevention performance of oil-containing silicone elastomers, *Sci. Rep.*, 2022, **12**, 11799.
- 91 D. Zhao, X.-D. Xu, S.-S. Yuan, S.-J. Yan, X.-H. Wang, S.-F. Luan and J.-H. Yin, Fouling-resistant behavior of liquid-infused porous slippery surfaces, *Chin. J. Polym. Sci.*, 2017, **35**, 887–896.
- 92 J. Liu, X. Xu, Y. Lei, M. Zhang, Z. Sheng, H. Wang, M. Cao, J. Zhang and X. Hou, Liquid Gating Meniscus-Shaped Deformable Magnetoelastic Membranes with Self-Driven Regulation of Gas/Liquid Release, *Adv. Mater.*, 2022, **34**, 2107327.
- 93 Z. Guo, D. Boylan, L. Shan and X. Dai, Hydrophilic reentrant SLIPS enabled flow separation for rapid water harvesting, *Proc. Natl. Acad. Sci.*, 2022, **119**, e2209662119.
- 94 K. Maji, A. Das, M. Dhar and U. Manna, Synergistic chemical patterns on a hydrophilic slippery liquid infused porous surface (SLIPS) for water harvesting applications, *J. Mater. Chem. A*, 2020, **8**, 25040–25046.
- 95 C. Wang, S. Wang, H. Pan, L. Min, H. Zheng, H. Zhu, G. Liu, W. Yang, X. Chen and X. Hou, Bioinspired liquid gating membrane-based catheter with anticoagulation and positionally drug release properties, *Sci. Adv.*, 2020, **6**, eabb4700.
- 96 K. Chae, W. Y. Jang, K. Park, J. Lee, H. Kim, K. Lee, C. K. Lee, Y. Lee, S. H. Lee and J. Seo, Antibacterial infection and immune-evasive coating for orthopedic implants, *Sci. Adv.*, 2020, **6**, eabb0025.
- 97 K. Park, S. Kim, Y. Jo, J. Park, I. Kim, S. Hwang, Y. Lee, S. Y. Kim and J. Seo, Lubricant skin on diverse biomaterials with complex shapes via polydopamine-mediated surface functionalization for biomedical applications, *Bioact. Mater.*, 2023, **25**, 555–568.
- 98 D. C. Leslie, A. Waterhouse, J. B. Berthet, T. M. Valentin, A. L. Watters, A. Jain, P. Kim, B. D. Hatton, A. Nedder, K. Donovan, E. H. Super, C. Howell, C. P. Johnson, T. L. Vu, D. E. Bolgen, S. Rifai, A. R. Hansen, M. Aizenberg, M. Super, J. Aizenberg and D. E. Ingber, A bioinspired omniphobic surface coating on medical devices prevents thrombosis and biofouling, *Nat. Biotechnol.*, 2014, **32**, 1134–1140.
- 99 H. Sun, R. Li, H. Li, Z. Weng, G. Wu, P. Kerns, S. Suib, X. Wang and Y. Zhang, Bioinspired Oil-Infused Slippery Surfaces with Water and Ion Barrier Properties, *ACS Appl. Mater. Interfaces*, 2021, **13**, 33464–33476.
- 100 B. Lemaire, Y. Yu, N. Molinari, H. Wu, Z. A. H. Goodwin, F. Stricker, B. Kozinsky and J. Aizenberg, Flexible fluid-based encapsulation platform for water-sensitive materials, *Proc. Natl. Acad. Sci.*, 2023, **120**, e2308804120.
- 101 H. Carrion, S. Joshi, R. Shirwaiker and S. Fonash, A novel fabrication method for embedding metal structures into polymers for flexible electronics, *62nd IIE Annual Conference and Expo 2012*, 2012, pp. 3212–3221.
- 102 S. Walker, J. Rueben, T. V. Volkenburg, S. Hemleben, C. Grimm, J. Simonsen and Y. Mengüç, Using an environmentally benign and degradable elastomer in soft robotics, *Int. J. Intell. Robot. Appl.*, 2017, **1**, 124–142.
- 103 J. Yang, J. Steck, R. Bai and Z. Suo, Topological adhesion II. Stretchable adhesion, *Extreme Mech. Lett.*, 2020, **40**, 100891.
- 104 E. Petrie, Cyanoacrylate Adhesives in Surgical Applications, *Rev. Adhes. Adhes.*, 2014, **2**, 253–310.
- 105 E. A. S. Marques, L. F. M. da Silva, M. D. Banea and R. J. C. Carbas, Adhesive Joints for Low- and High-Temperature Use: An Overview, *J. Adhes.*, 2015, **91**, 556–585.
- 106 K. Pan, X. Zeng, H. Li and X. Lai, Synthesis of silane oligomers containing vinyl and epoxy group for improving the adhesion of addition-cure silicone encapsulant, *J. Adhes. Sci. Technol.*, 2016, **30**, 1131–1142.
- 107 D. G. Barrett, G. G. Bushnell and P. B. Messersmith, Mechanically robust, negative-swelling, mussel-inspired tissue adhesives, *Adv. Healthcare Mater.*, 2013, **2**, 745–755.
- 108 D. Gan, W. Xing, L. Jiang, J. Fang, C. Zhao, F. Ren, L. Fang, K. Wang and X. Lu, Plant-inspired adhesive and tough hydrogel based on Ag-Lignin nanoparticles-triggered dynamic redox catechol chemistry, *Nat. Commun.*, 2019, **10**, 1487.
- 109 X. Wei, K. Ma, Y. Cheng, L. Sun, D. Chen, X. Zhao, H. Lu, B. Song, K. Yang and P. Jia, Adhesive, Conductive, Self-Healing, and Antibacterial Hydrogel Based on Chitosan–Polyoxometalate Complexes for Wearable Strain Sensor, *ACS Appl. Polym. Mater.*, 2020, **2**, 2541–2549.
- 110 R. Liu, Y. Li, J. Chen, X. Zhang, Z. Niu and Y. Sun, The preparation of multifunction chitosan adhesive hydrogel by “one- step” method, *J. Biomater. Sci., Polym. Ed.*, 2020, **31**, 1925–1940.
- 111 X. Shi and P. Wu, A Smart Patch with On-Demand Detachable Adhesion for Bioelectronics, *Small*, 2021, **17**, 2101220.
- 112 W. Liu, R. Xie, J. Zhu, J. Wu, J. Hui, X. Zheng, F. Huo and D. Fan, A temperature responsive adhesive hydrogel for fabrication of flexible electronic sensors, *npj Flexible Electron.*, 2022, **6**, 68.





- 113 X. Jiang, F. Zeng, L. Zhang, A. Yu and A. Lu, Engineered Injectable Cell-Laden Chitin/Chitosan Hydrogel with Adhesion and Biodegradability for Calvarial Defect Regeneration, *ACS Appl. Mater. Interfaces*, 2023, **15**, 20761–20773.
- 114 Y. Zhang, Y. Dai, F. Xia and X. Zhang, Gelatin/polyacrylamide ionic conductive hydrogel with skin temperature-triggered adhesion for human motion sensing and body heat harvesting, *Nano Energy*, 2022, **104**, 107977.
- 115 X. Peng, X. Xu, Y. Deng, X. Xie, L. Xu, X. Xu, W. Yuan, B. Yang, X. Yang, X. Xia, L. Duan and L. Bian, Ultrafast Self-Gelling and Wet Adhesive Powder for Acute Hemostasis and Wound Healing, *Adv. Funct. Mater.*, 2021, **31**, 33.

